ISSN: 1983 7402 ITA, 27 a 29 SET 2022

Influence of Cosmic Radiation on RF Signal Envelope Detectors Assisted by Microwave Photonics on Board CubeSats

André Paim Gonçalves[1], Felipe Streitenberger Ivo[1], Olympio Lucchini Coutinho[1], Felipe Araújo Marins[2], Heitor Albuquerque[2], Ricardo Marques Ribeiro[3]
[1]Instituto Tecnológico de Aeronáutica (ITA), São José dos Campos/SP – Brasil
[2]Instituto de Pesquisa da Marinha (IPqM), Rio de Janeiro/RJ– Brasil
[3]Universidade Federal Fluminense (UFF), Niterói/RJ– Brasil

***Abstract* – This paper intends to make a brief analysis of the influence of cosmic radiation on RF signal envelope detectors implemented by Microwave Photonics (MWP) techniques on board CubeSats. Such satellites are of small size, can operate in low altitude orbit, and have very stringent requirements regarding electrical power consumption, volume, and weight. Receivers based on envelope detectors assisted by MWP are candidates for boarding CubeSats. Such receivers that employ Bragg gratings recorded on silica optical fiber are influenced by cosmic radiation that shifts the Bragg resonance frequency. This work proposes a numerical analysis from data obtained in the literature to simulate the photonic RF receiver behavior under the influence of a 2 krad cosmic radiation load accumulated over two years corresponding to the satellite operation in low orbit. The accumulated cosmic radiation, for these conditions, can cause a 2 pm wavelength shift of the Bragg grating resonance, which does not impact the photonic RF receiver.**

***Keywords* – Cosmic radiation impact, RF receiver assisted by microwave photonics, CubeSat.**

I. INTRODUCTION

The use of low-orbit, small satellites that can operate radar and communication systems is interesting for dual applications, that is, both in operational applications for the Armed Forces and in civilian applications like deforestation, agriculture, relays, and other uses [1].

The satellites called CubeSats are small, operate in low orbit, and have very stringent requirements regarding consumption, volume, weight, and operating bandwidth. It should be pointed out, that CubeSats due to their requirements can employ receivers based on MWP-assisted RF signal envelope detectors, this idea is schematically shown in Fig. 1. These receivers rely on the use of optical fiber and other optical devices that have characteristics related to low consumption, weight, and volume, as well as large RF bandwidth [1]. Many CubeSats have the proposal to internally employ off-the-shelf electronic devices, that is, devices found for non-space applications [1]. This reduces design costs. However, these electronic circuits have not been prepared to operate in environments with large temperature variations and high exposure to cosmic radiation.

For the correct use of electronic and photonic devices, it must be considered that a successful space mission requires that the components, and consequently the onboard systems, work correctly during the entire duration of the mission. Regarding satellites, there is no room for error, because once launched, few repairs are possible [2]. All systems must be certified as early as the development phase of the project. In general, for each mission, the degree of reliability in the systems is dependent on several factors, such as the duration of the mission, the environment in which it will take place, the availability of budget, and other criteria. For observation or telecommunication satellites their lifetime varies from 3 to 10 years [1]. Because the lifespan of this type of satellite is shorter than that of other types, there is relaxation concerning the intemperate nature of the space environment.

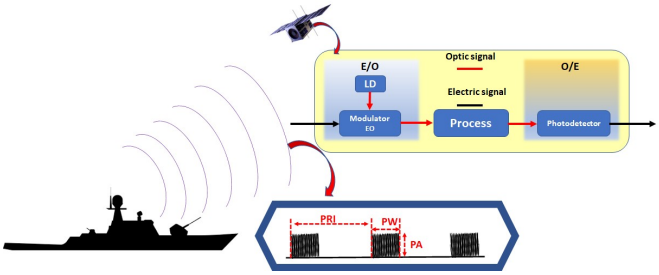

Fig. 1. Schematic diagram of photonic receiver boarding in CubeSat, which is receiving RF signals from a ship. LD – Laser Diode; PRI – Pulse Repetition Interval; PW – Pulse Width; PA – Pulse Amplitude; E/O - Electric/Optic converter; and O/E - Optic/Electric converter.

For this work, an electromagnetic spectrum surveillance satellite that employs a low orbit will be considered. Its altitude may vary between 700 to 1000 km. More specifically, the satellite operates in heliosynchronous orbit at an altitude of 778 km, performs 14 revolutions per day, and has a mission duration of two years. Given these assumptions, the study was conducted considering a photonic RF receiver based on a uniform Bragg grating. This device, which is composed of silica fiber and passive devices, suffers the influence of ionizing radiation from the space environment for these attitudes [2]. However, this work focuses on cosmic radiation influence in receiver tunning.

This paper considers a fully photonic RF receiver architecture based on an optical self-homodyne technique to detect RF emissions as was reported in [3]. An optical self-homodyne detection technique is a process that a single–sideband–suppressed carrier (SSB-SC) is directly photodetected. When the optical signal is modulated by an RF signal and becomes an SSB-SC, the result is an RF power conversion to a baseband voltage signal proportional to the original input signal that modulates the RF sub-carrier.

The Bragg grating is the component of the optical circuit responsible for converting the modulated optical signal into an SSB-SC signal. The optical envelope detector depends on the tuning of the signal with respect to the Bragg grating rejection range. Cosmic radiation, especially gamma rays, can cause the Bragg grating resonance frequency shift and it

can influence the sensitivity of the photonic envelope detector.

In order to verify the influence of gamma radiation on the photonic envelope detector, a study was conducted on the impact of this radiation on Bragg gratings. Some works that emulate the space environment with the use of Cobalt-60 (Co-60) were analyzed, as well as the use of the software SPENVIS (The Space Environment Information System) which calculates the annual cumulative dose of ionizing radiation on Silicium. The wavelength shift caused by the ionizing radiation was estimated to verify the tunning Bragg influence on the sensibility of the photonic envelope detector. The sensitivity value, even with the influence of gamma radiation, was the same value observed in [3]. It is a measured sensitivity system of 53 kV/W for an RF range of 10 to 20 GHz.

II. SYSTEM CONFIGURATION AND PRINCIPLE OF THE PHOTONIC RF RECEIVER

The principle of operation of the fully photonic RF receiver is based on the optical self-homodyne detection as is shown in Fig. 2. The laser light wave is coupled to the phase modulator and undergoes optical phase modulation by the RF signal. The modulated optical signal passes through an optical filter. The optical carrier and the lower sideband of the modulated signal are rejected by the optical filter. The upper sideband portion of the modulated optical signal is transmitted through the filter to the photodetector. As a result, the upper sideband is converted into a baseband electrical signal by direct detection, i.e. none interferometer is used before detection. This process is similar to the one used in [4], where the authors presented this structure, see Fig.2, as a down converter receiver.

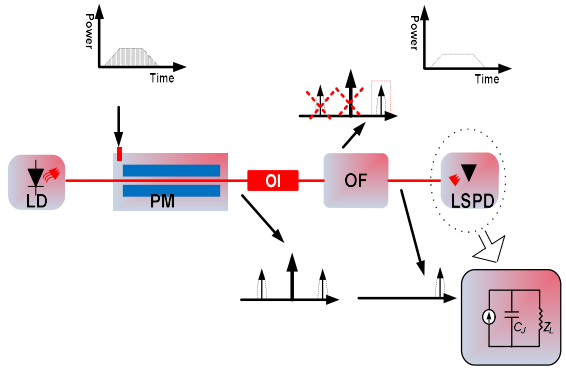

Fig. 2. Schematic diagram of the photonic ED. LD – Laser Diode, PM – Phase Modulator, OI – Optical Isolator, OF – Optical Filter, LSPD – Low-Speed Photodetector, C_J – Junction Capacitance, and Z_L - Output Load.

This optical circuit uses an optical phase modulator to modulate the carrier with the RF radar input signal, and the phase-to-intensity (PM-IM) modulation conversion technique by optical filtering [5]. Traditionally, the PM-IM conversion is achieved by filtering one of the optical modulated sidebands using fiber Bragg grating (FBG). When the optical carrier is preserved, the beating between it and the remaining optical sideband components will result in a filtered RF signal at the photodetector output [5]. To achieve optical self-homodyne in this work, the optical carrier is tuned to be filtered together with the rejected sideband portion, this process is shown in Fig. 3. So, only the non-rejected sideband phase-modulated spectrum reaches the PD. If the RF signal is pulsed, the beating among the optical components at the PD produces an RF pulse envelope detection at the system output. When the optical carrier power of the phase-modulated signal is filtered, it is possible to increase the optical signal power at the system input without saturating the photodetector. This allows more power to be transferred from the optical signal to the RF signal, increasing the dynamic range of the system.

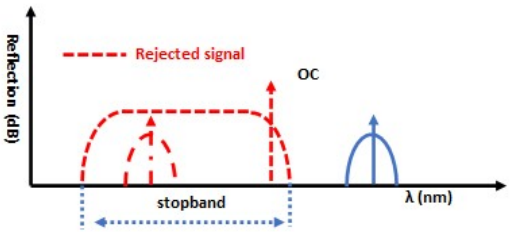

Fig. 3: Behavior of the ideal optical filter and the optical carrier tuning. OC – Optical Carrier.

The system architecture implementation is quite simple using an optical PM at the RF input and a low-cost and low-speed photodetector at the output. Different from MWP architecture that uses Mach-Zehnder (MZM) intensity modulator, the proposed architecture does not need modulator bias voltage control. As the photodetection is performed at the baseband frequency spectrum, the only microwave electric circuit is the PM input [3].

However, if the input is a pulsed RF signal, the RF envelope detection can be also performed directly on the photodetector using the same optical self-homodyne technique [3], [4] as was explained in the previous paragraph. By using photonic RF envelope detection, the expensive high-speed photodetector at the system output is no longer needed, as well as any kind of microwave frequency electronic circuit. Additionally, when the photodetector is operating at a low-frequency baseband, it is possible to achieve transimpedance gain just by increasing the load impedance output [3].

The important process to consider in the proper operation of this receiver is the RF signal amplification by power transferred from the optical circuit to the RF signal envelope with transimpedance gain contribution. Combining the optical and the transimpedance gain contribution, it is demonstrated 53 kV/W of system sensitivity for an RF range of 10 to 20 GHz [3].

A. Impact of Gamma Radiation on the Bragg Grating

Uniform fiber Bragg gratings can employ standard commercially available single mode corning SMF-28 fibers. They are doped with Germanium (Ge) in order to increase the

refractive index of the core thus guiding the light and at the same time, the Ge doping increases the laser photosensitivity at ultraviolet wavelengths for Bragg grating recording. In this process, Hydrogen atoms may be inserted (hydrogen-loading) to increase the photosensitivity and thus the refractive index contrast [6].

The simulation of the radiation environment in space is difficult to achieve in the laboratory because there is a combination of several types of radiation and their interactions with the structural materials present, e.g. aluminum, plastic, rubber, and others. In addition, the energy spectra obtained in the laboratory most often represent only discrete bands of the total spectrum. These ground-based simulations provide results that must be factored for representativeness in space. Tests that can provide information regarding Total Dose Effects can be performed with isotopic gamma ray sources, for example Co-60.

With the exposure of this grating to gamma radiation, the refractive index changes and thereby the wavelength of maximum reflection of the grating will shift.

To minimize the effect of cosmic radiation on the grating degradation inside the satellite, it is possible to use aluminum absorber shields with special paints [2]. However, as thicker bulkheads and/or paints are placed, the satellite will have increased weight. This increase in weight can cause, for example, more consumption of fuel for orbit correction, thus reducing its useful life. Using Space ENVironment Information System - SPENVIS software to calculate the dose accumulated in a silicon component on a Cubesat for one year in a heliosynchronous orbit at an altitude of 778 km, with 14 revolutions per day and with a 5 mm aluminum shield. The cumulative dose is shown in Fig. 4**.**

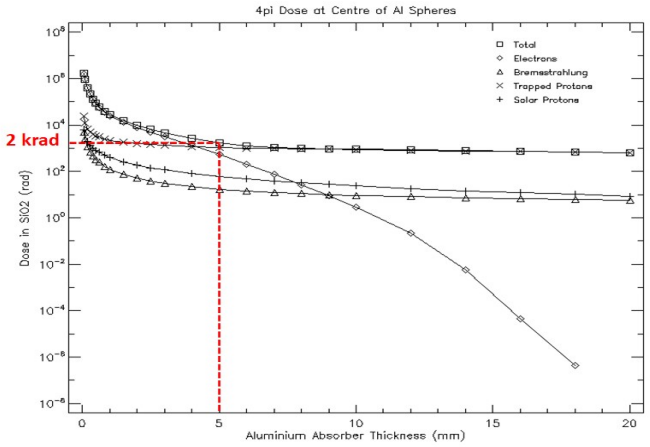

Fig. 4. Radiation dose in rad during two years of heliosynchronous orbit for the satellite calculated by SPENVIS.

In Fig. 4 it is observed that the thickness of the aluminum absorber of the order of 5 mm is sufficient to shield the electronic and photonic components in order to reduce the radiation dose to the minimum to be received. This is because the curves saturate from about 5 mm thickness, i.e. any value above this would cause an unnecessary increase in weight.**,**

As there is a prediction of an approximate value of total accumulated radiation on account of this bulkhead. This value is used as reference to achieve the Bragg grating wavelength shift. Given the application of the Total Ionizing Dose (TID) test using Cobalt-60 (Co-60) [2]. Many studies have been done on the effects of ionizing gamma radiation and its natural source to the fiber optic circuits inside the spaceflight environment. Information can be found in the literature regarding the dependence of the performance of fiber in a radiation environment on the materials, the processes, the coatings used in its making, the dose type, the rate, and the total dose. Recovery times, self-annealing, and the effects of photobleaching have also been well documented.

Manufacturers interested in the spaceflight market are aware of these dependencies and have developed manufacturing processes for products that can withstand tens to hundreds of total dose krads, with an increase of less than one dB of loss per kilometer of fiber [7]–[9]. The optical fiber will "darken" due to ionizing radiation, that is, because of the creation of absorption centers, where unwanted chemical elements and other optical defects will settle in that fiber. Generally, a fiber will suffer defects during the production process making them difficult to isolate and eliminate, regardless of the purity of the glass preform [7]–[9].

For the case of Bragg gratings, Germanium is used to dope the fiber core to increase the refractive index of the waveguide during the recording of the grating, this is due to the increased sensitivity to radiation. It should be noted that Phosphorus when acting as a dopant for the fiber core or cladding is not acceptable for use in space environments [4].

At controlled temperatures because the CubeSat temperature protection, the annealing of the color centers does not occur. In general, it is best to use pure silica in space applications when the total dose requirements exceed 5 krads [5].

To check how the Bragg gratings recorded on commercial optical fibers behave under gamma ray irradiation, three commercially available optical fibers Bragg gratings were chosen. in the corning SMF-28 standard, from three different optical fiber manufacturers (AOS, Germany; Business Unitec, Russia, and CRC, Canada). The results are shown in Fig. 5 [10].

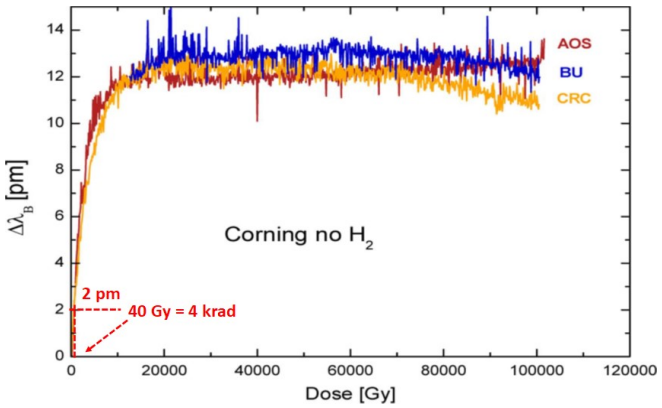

Fig. 5. Variation of the wavelength of maximum reflection of the grating (λ_B) as a function of the radiation dose in Gray unities [Gy], it should be noted that 10 Gy = 1000 rad [10].

The behavior observed in Fig. 5 shows that dosages around 4 krad or 40 Gy provide a displacement of the Bragg resonance to 2 pm. A displacement of the Bragg resonance of 2 pm is equivalent to a frequency displacement of about 250 MHz. As the satellite is expected to operate for two years and as the temperature for this study is considered constant and well defined, it is possible to infer that the dose of accumulated gamma radiation reaches values around of 40 Gy. For this dose, an equivalent Bragg grating shift is 2 pm.

III. EXPERIMENTAL VERIFICATION OF THE GAMMA RADIATION IMPACT ON PHOTONIC ENVELOPE DETECTOR

To verify the gamma radiation impact on the photonic envelope detector, an experiment was carried out. The Bragg wavelength shift was emulated with a proportional laser wavelength displacement.

A DFB laser is used as an optical source. The phase modulator operates at frequencies up to 20 GHz. A uniform FBG is used as an optical filter followed by a 1.5 GHz low-speed photodetector. The RF signal generator performs the RF pulsed signal. A high-speed digital sampling oscilloscope (DSO) measures the input RF modulated signal and the output video signal, that is, the envelope of the input signal. The schematic diagram shows this experimental approach in Fig. 6.

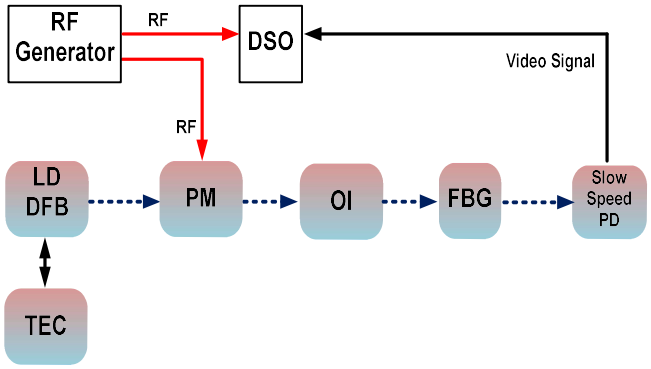

Fig. 6: Schematic diagram setup of the receiver. DFB - Distributed Feedback Laser, TEC - Thermal Electronic Cooler, PM – Phase Modulator; OI - Optical Isolator, RF - Radio Frequency, PD - Photodetector, and FBG - Fiber Bragg Grating.

The rejection band of the optical filter is shown in Fig. 7. This figure shows the right cut on the center frequency. The left side is symmetric to the right side. The right edge has a roll-off starting from the region's maximum optical signal reflection and ending at the total transmission.

The transition region between stopband and transmission band has a roll-off around 2.86 dB/GHz. This imposes a limitation on the RF flatness response operation band, starting at wavelength equivalent to 10 GHz from the laser carrier wavelength, considering the laser carrier tuned at the right edge frequency of the optic stopband.

The DFB laser operates at a frequency of around 193.23 THz by optical cavity temperature adjusting. To achieve optical self-homodyne in this work, the optical carrier is tuned to be filtered together with the rejected lower sideband portion as shown in Fig. 7.

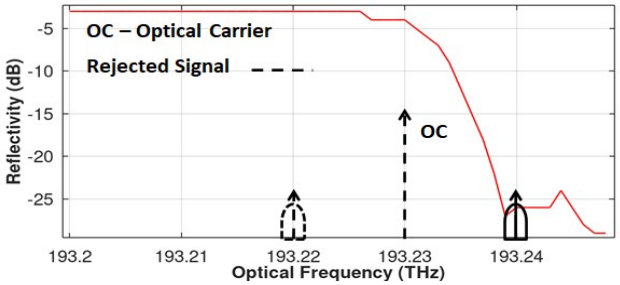

Fig. 7: Right side of optical filter rejection band. This stopband center frequency is approximately around 193.200 THz.

To achieve the dynamic range, an RF pulsed radar signal was set with a pulse width (PW) equal to 4 ms and a pulse repetition interval (PRI) of 10 ms.

The system sensitivity test relied on pulsed RF signals generated with the carrier varying from 10 to 20 GHz. The RF signal was generated with power variation from -10 to 16 dBm. A photodetector saturation process occurs from -3.3 to 16 dBm as shown in Fig. 8 (a) and (b) respectively. The RF power value of 16 dBm was chosen from the information of the maximum RF power supported at the PM input. The output voltage value was 25 V for -3.3 and 16 dBm as shown in Fig. 8 (c) and (d) respectively.

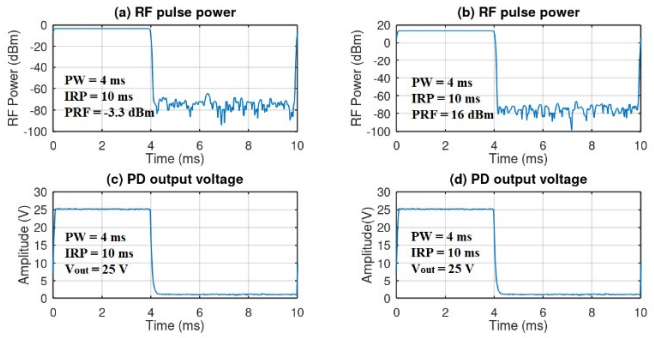

Fig. 8: Measured input and output radar pulses. RF input pulse powers at 10 GHz are shown in (a) and (b). The output PD voltage is shown in (c) and (d). The PD load resistance is 500 kΩ.

In Fig. 8 (c) and (d), the pulsed signal can be seen undistorted and with its envelope measured with the flattened voltage value equal to 25 V. The output voltage of the system remains at the same value without increase. The input carrier frequency was varied from 10 to 20 GHz, the same results of sensitivity were achieved for all this frequency**.** This fact shows that the system's upper power detecting limit is -3.3 dBm. Using a system sensitivity concept, its value is achieved by dividing the video voltage value by the RF input power. The system sensitivity value is calculated as 25 V/(-3dBm) = 25V/(0.5 mW) = 50 kV/W ~ 53 kV/W in the 10-20 GHz frequency range.

To check the gamma radiation impact on the photonic receiver, a laser wavelength shift value of 2 pm was used relating to upper edge of the FBG stopband to emulate a

Bragg wavelength shift of 2 pm. The experimental approach used is the same observed in Fig. 6. The measured system sensitivity is 53 kV/W for all frequency range from 10 to 20 GHz.

IV. CONCLUSION

The use of RF signal receivers on satellites that operate in low orbits can bring operational gains for the Armed Forces and other dual activities such as agriculture, deforestation, and others. However, shipping RF signal receivers to satellites require a lot of energy and space. One solution to this problem would be the use of Microwave Photonics. This work sought to make a simplified approach to the behavior of a photonic RF signal receiver based on Bragg grating under the influence of the cosmic rays environment. In this study it was observed that the employment of these receivers has its performance dependent on the material used to build electronic and photonic circuits, the type and thickness of the employed shield and radiation dose for which the satellite is exposed. As the operation of CubeSat satellites can last from 3 to 10 years, it was possible to estimate a cumulative dose over this period and verify its influence. It was considered that this dose would shift the Bragg grating reflective peak response by 2 pm. This spectral shift was not able to modify the predicted sensitivity of 53 kV/W when the system is free from ionizing radiation incidence.

REFERENCES

[1] D. Muhire, D. Stepanova, K. Bhale, M. Chakraborty, and D. Wischert, “A review of near future optical technology for high-speed and secure CubeSat communications,” Dec. 2021.

[2] Claro, L. Henrique; Santos, J. Antonio, “Danos de radiação em componentes eletrônicos nas aplicações aeroespaciais,” 2005.

[3] A. P. Gonçalves, F. S. Ivo, and O. L. Coutinho, “High sensitivity envelope detector assisted by microwave photonics,” in *2021 SBMO/IEEE MTT-S International Microwave and Optoelectronics Conference (IMOC)*, 2021, pp. 1–3, doi: 10.1109/IMOC53012.2021.9624769.

[4] M. Hossein-Zadeh and A. F. J. Levi, “Selfhomodyne photonic microwave receiver architecture based on linear optical modulation and filtering,” *Microw. Opt. Technol. Lett.*, vol. 50, no. 2, pp. 345–350, 2008, doi: 10.1002/mop.23065.

[5] C. Wang and J. Yao, “Fiber Bragg gratings for microwave photonics subsystems,” *Opt. Express*, vol. 21, no. 19, pp. 22868–22884, 2013, doi: 10.1364/OE.21.022868.

[6] and D. A. R. Kashyap, P. F. Mckee, “UV written reflection grating structures in photosensitive optical fibers using phase-shifted phase masks,” *Electron. Lett.*, vol. 30, no. 23, pp. 1977–1978, 1994.

[7] E. J. Friebele, “Photonics in the space environment,” 1991.

[8] *Handbook of radiation effects*. United States: Oxford University Press Inc, 1993.

[9] M. Ott and J. Plante, “Fiber Optic Cable Assemblies for Space Flight Applications: Issues and Remedies,” Mar. 1997, doi: 10.2514/6.1997-5592.

[10] S. K. Hoeffgen *et al.*, “Comparison of the Radiation Sensitivity of Fiber Bragg Gratings Made by Four Different Manufacturers,” *IEEE Trans. Nucl. Sci.*, vol. 58, no. 3, pp. 906–909, 2011, doi: 10.1109/TNS.2011.2106800.